frontiers in Veterinary Science

ORIGINAL RESEARCH
published: 26 October 2021
doi: 10.3389/fvets.2021.771726

Pulmonary Vascular Resistance Estimated by Echocardiography in Dogs With Myxomatous Mitral Valve Disease and Pulmonary Hypertension Probability

Ryohei Suzuki†, Yunosuke Yuchi†, Haruka Kanno, Takahiro Saito, Takahiro Teshima, Hirotaka Matsumoto and Hidekazu Koyama*

Laboratory of Veterinary Internal Medicine, Faculty of Veterinary Medicine, School of Veterinary Science, Nippon Veterinary and Life Science University, Musashino, Japan

OPEN ACCESS

Edited by:
Anusak Kijtawornrat, Chulalongkorn University, Thailand

Reviewed by:
Sirilak Disatian Surachetpong, Chulalongkorn University, Thailand
Nakkawee Saengklub, Mahidol University, Thailand

***Correspondence:**
Ryohei Suzuki
ryoheisuzuki@nvlu.ac.jp

†*These authors have contributed equally to this work and share first authorship*

Specialty section:
This article was submitted to Comparative and Clinical Medicine, a section of the journal Frontiers in Veterinary Science

Received: *07 September 2021*
Accepted: *29 September 2021*
Published: *26 October 2021*

Citation:
Suzuki R, Yuchi Y, Kanno H, Saito T, Teshima T, Matsumoto H and Koyama H (2021) Pulmonary Vascular Resistance Estimated by Echocardiography in Dogs With Myxomatous Mitral Valve Disease and Pulmonary Hypertension Probability. Front. Vet. Sci. 8:771726. doi: 10.3389/fvets.2021.771726

Post-capillary pulmonary hypertension (PH) is a life-threatening complication in dogs with myxomatous mitral valve disease (MMVD). An increase in pulmonary vascular resistance (PVR) is associated with post-capillary PH progression. In humans, PVR estimated by echocardiography (PVRecho) enables the non-invasive assessment of PVR in patients with PH. This study aimed to evaluate the clinical utility of PVRecho in dogs with MMVD, PH probability, and right-sided congestive heart failure (R-CHF). Dogs with MMVD and detectable tricuspid valve regurgitation were included in the study. Dogs were classified into three PH probability groups (low/intermediate/high) and according to the presence or absence of R-CHF. All dogs underwent echocardiographic measurements for right ventricular (RV) morphology and function. PVRecho was calculated by two methods using tricuspid valve regurgitation velocity and velocity–time integral of the pulmonary artery flow (PVRecho and PVRecho2). RV size indicators were significantly higher with a higher probability of PH. RV strain and velocity–time integral of the pulmonary artery flow in the high probability group were significantly lower than those in the other groups. Tricuspid valve regurgitation velocity, PVRecho, and PVRecho2 were significantly higher with an increase in PH probability. Logistic regression analysis revealed a significant association between the presence of R-CHF and increased PVRecho2 and end-diastolic RV internal dimension normalized by body weight. PVRecho and PVRecho2 showed significant differences among the PH probability groups. These non-invasive variables may be useful for the diagnosis and stratification of PH and the determination of the presence of R-CHF in dogs with MMVD.

Keywords: canine, combined post- and pre-capillary pulmonary hypertension, congestive heart failure, post-capillary pulmonary hypertension, pulmonary arterial pressure, pulmonary vascular remodeling, right ventricular adaptation, tricuspid regurgitation

INTRODUCTION

Pulmonary hypertension (PH) is a life-threatening disease in dogs and is characterized by an increase in pulmonary arterial pressure (PAP) and/or pulmonary vascular resistance (PVR) (1, 2). PH is induced by various diseases in dogs, including pulmonary arterial disease, left heart disease, respiratory disease, hypoxia, pulmonary embolic disease, parasitic disease, or a combination of these (1). In particular, PH secondary to left heart disease is called post-capillary PH because the main factor of increasing PAP is considered to be the increased pulmonary venous pressure; it is classified into two subtypes: isolated post-capillary PH (Ipc-PH) and combined post- and pre-capillary PH (Cpc-PH) (1, 3–5). The former is caused solely by pulmonary venous congestion due to increasing left atrial pressure, whereas the latter is caused by the increase in PVR associated with pulmonary vascular remodeling in addition to the pathophysiology of Ipc-PH. As a result, the PAP in Cpc-PH was higher than that in Ipc-PH. Recent human studies have reported that Cpc-PH is significantly associated with poor prognosis in patients with left heart disease and heart failure (6–8). Therefore, PVR assessment is essential to determine the pathophysiology and prognosis of dogs with post-capillary PH.

The gold standard for determining the disease state of PH is by right heart catheterization (1, 9). Additionally, the absolute evaluation of PVR requires a catheterization-derived cardiac output and transpulmonary pressure gradient. However, the availability of right heart catheterization is limited, and its clinical use is restricted due to the need for anesthesia. Therefore, echocardiography has been used as an alternative to invasive indicators for disease evaluation. Specifically, in humans, PVR is estimated by echocardiography (PVRecho), which is calculated using tricuspid valve regurgitation (TR) velocity and the velocity–time integral of the pulmonary artery flow (PV VTI), has been reported to identify patients with elevated PVR (10–13). However, to the best of our knowledge, only one study has assessed the clinical utility of PVRecho in veterinary medicine (14).

The primary objective of this study was to evaluate the clinical utility of PVRecho in dogs with myxomatous mitral valve disease (MMVD), the most common cardiac disease in dogs (15). We hypothesized that PVRecho might provide additional information for the diagnosis and pathophysiological evaluation of PH in dogs with MMVD.

Abbreviations: 2D-STE, two-dimensional speckle tracking echocardiography; 3seg, only right ventricular free wall analysis; 6seg, right ventricular global analysis; CI, confidence interval; CV, coefficient of variation; ICC, intra- or inter-class correlation coefficients; MMVD, myxomatous mitral valve disease; PA/Ao, pulmonary artery to aortic diameter ratio; PAP, pulmonary arterial pressure; PH, pulmonary hypertension; PVR, pulmonary vascular resistance; PVRecho, pulmonary vascular resistance estimated by echocardiography; PV VTI, velocity-time integral of the pulmonary artery flow; RV, right ventricular; RV FACn, right ventricular fractional area change normalized by body weight; RV MPI, right ventricular myocardial performance index; RV s', tissue Doppler imaging-derived peak systolic myocardial velocity of lateral tricuspid annulus; RVEDA index, end-diastolic right ventricular area normalized by body weight; RVESA index, end-systolic right ventricular area normalized by body weight; RVIDd index, end-diastolic right ventricular internal dimension normalized by body weight; RV-SL, right ventricular longitudinal strain; RV-SrL, right ventricular longitudinal strain rate; TAPSEn, tricuspid annular plane systolic excursion normalized by body weight; TR, tricuspid valve regurgitation.

MATERIALS AND METHODS

This was a prospective observational study. Client-owned dogs that underwent cardiac screening at the Nippon Veterinary and Life Science University Veterinary Medical Teaching Hospital were recruited from October 2017 to May 2019. All procedures followed the Guidelines for Institutional Laboratory Animal Care and Use of Nippon Veterinary and Life Science University in Japan, and the study was approved by the Ethical Committee for Animal Use of the Nippon Veterinary and Life Science University Veterinary Medical Teaching Hospital, Japan (approval number: R2-5). Written informed consent authorizing the participation of the dogs in this study was obtained from all dog owners.

Animals

Client-owned dogs with MMVD and detectable TR were prospectively included in our study. All dogs underwent complete physical examination, electrocardiography, blood pressure measurement by oscillometric method, and radiographic and echocardiographic examinations. Dogs were diagnosed as having MMVD based on echocardiographic findings of mitral valve thickening, prolapse, and mitral regurgitation (16, 17). Clinical diagnosis of TR was performed by inspecting the tricuspid valve from multiple views and using color Doppler echocardiography, and the peak TR velocity was obtained using the continuous-wave spectral Doppler method. Dogs that met the following criteria were excluded from the study: other cardiac diseases, diseases that might increase the PAP, such as pulmonary disease, thromboembolic disease, and neoplastic disease; diseases that might affect cardiac function, such as endocrine disease and systemic hypertension (systolic blood pressure $\geq$160 mmHg) (18), and/or missing data.

Classification

Dogs with MMVD were divided into three groups (Stage B1, B2, and C/D) based on the MMVD severity noted by the American College of Veterinary Internal Medicine (ACVIM) consensus (15). Additionally, dogs were classified according to the PH probability noted on the ACVIM consensus using echocardiographic findings of the TR velocity and anatomical abnormalities of the right heart, pulmonary artery, and caudal vena cava into low, intermediate, and high probability groups (1). Furthermore, dogs with MMVD were classified by the presence or absence of right-sided congestive heart failure (R-CHF). Dogs were diagnosed as having R-CHF if they had ultrasonographic and/or radiographic findings indicative of ascites, pleural effusion, or pericardial effusion without any abnormalities other than PH that may have been responsible (17).

Echocardiographic Evaluation of Right Heart

Conventional, two-dimensional, and Doppler echocardiographic examinations were performed using an echocardiographic

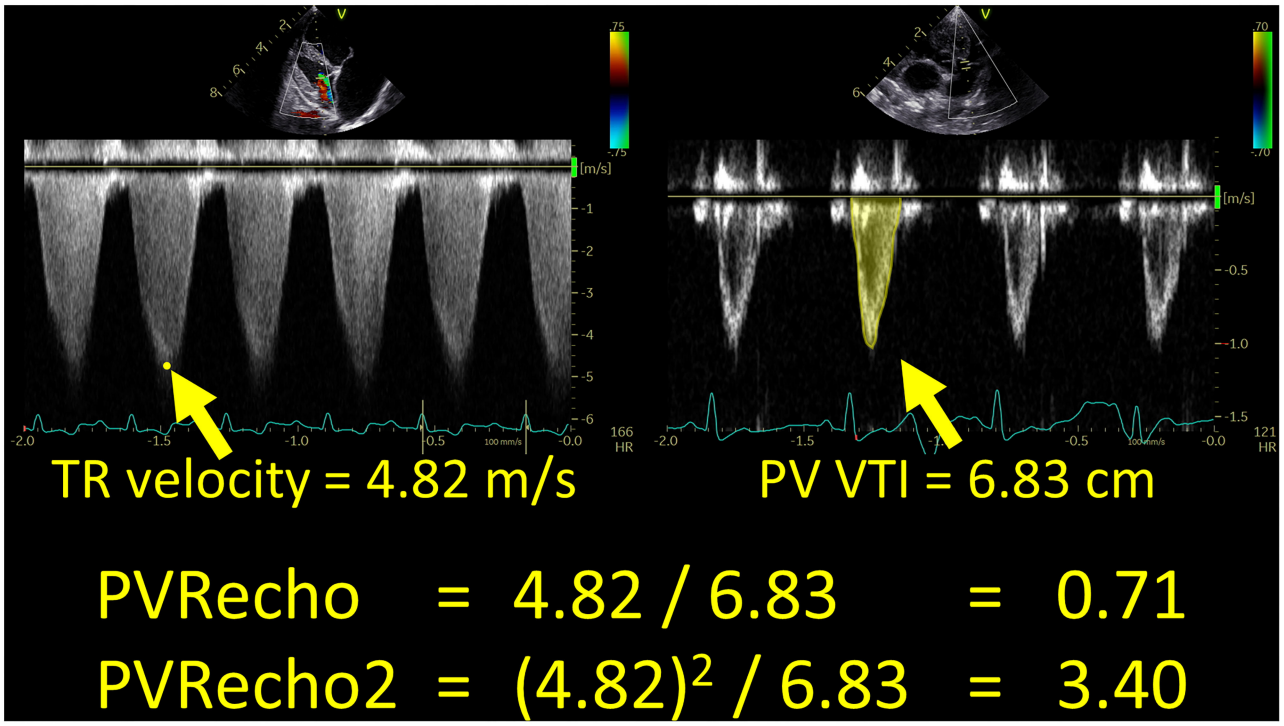

FIGURE 1 | Echocardiographic estimation of pulmonary vascular resistance in a dog with high pulmonary hypertension probability. PV VTI, velocity–time integral of the pulmonary artery flow; PVRecho, pulmonary vascular resistance estimated by echocardiography; TR, tricuspid valve regurgitation.

system (Vivid E95, GE Healthcare, Tokyo, Japan) and a 3.5–6.9 MHz transducer by a single investigator (RS). Lead II electrocardiography was recorded simultaneously, and the results are displayed on the images. Non-sedated dogs that were manually restrained in right and left lateral recumbency. All data were obtained from at least five consecutive cardiac cycles in sinus rhythm. All images were analyzed by a single observer (YY) who was well trained by a cardiologist using an offline workstation (EchoPAC PC, Version 204, GE Healthcare, Tokyo, Japan).

All echocardiographic variables were measured using five consecutive cardiac cycles in sinus rhythm from high-quality images. To evaluate the right ventricular (RV) morphology, end-diastolic RV internal dimension (RVIDd) and end-diastolic and end-systolic RV area (RVEDA and RVESA, respectively) were measured using the left apical four-chamber view optimized for the right heart (RV focus view) (17, 19–22). RVIDd was measured as the largest diameter at the middle RV, parallel to the tricuspid annulus, using the B-mode method (17). RVEDA and RVESA were measured by tracing the endocardial border of the RV inflow region at end-diastole and end-systole, excluding the papillary muscles. These variables were normalized by body weight using the following formulas (21):

$$\text{RVIDd index} = \frac{\text{RVIDd (mm)}}{[\text{body } \textit{weight} \text{ (kg)}]^{0.327}} \quad (1)$$

$$\text{RVEDA index} = \frac{\text{RVEDA (cm}^2\text{)}}{[\text{body weight (kg)}]^{0.624}} \quad (2)$$

$$\text{RVESA index} = \frac{\text{RVEDA (cm}^2\text{)}}{[\text{body weight (kg)}]^{0.628}} \quad (3)$$

Pulmonary artery to aortic diameter ratio (PA/Ao) was also obtained using the right parasternal short-axis view at the level of the heart base, as described previously (23).

For the RV functional assessment, tricuspid annular plane systolic excursion (TAPSE), RV functional area change (RV FAC), tissue Doppler imaging-derived peak systolic myocardial velocity of the lateral tricuspid annulus (RV s'), RV myocardial performance index (RV MPI), and PV VTI were measured as described previously (21–24). All RV functional indices, except PV VTI, were obtained using the RV focus view. The TAPSE was measured using the B-mode method, as described previously (17, 25). The TAPSE and RV FAC were normalized by body weight using the following formulas (25, 26):

$$\text{TAPSEn} = \frac{(\text{TAPSE [cm]})}{(\text{body weight [kg]})^{0.284}} \quad (4)$$

$$\text{RV FACn} = \frac{(\text{RV FAC [\%]})}{(\text{body weight [kg]})^{-0.097}} \quad (5)$$

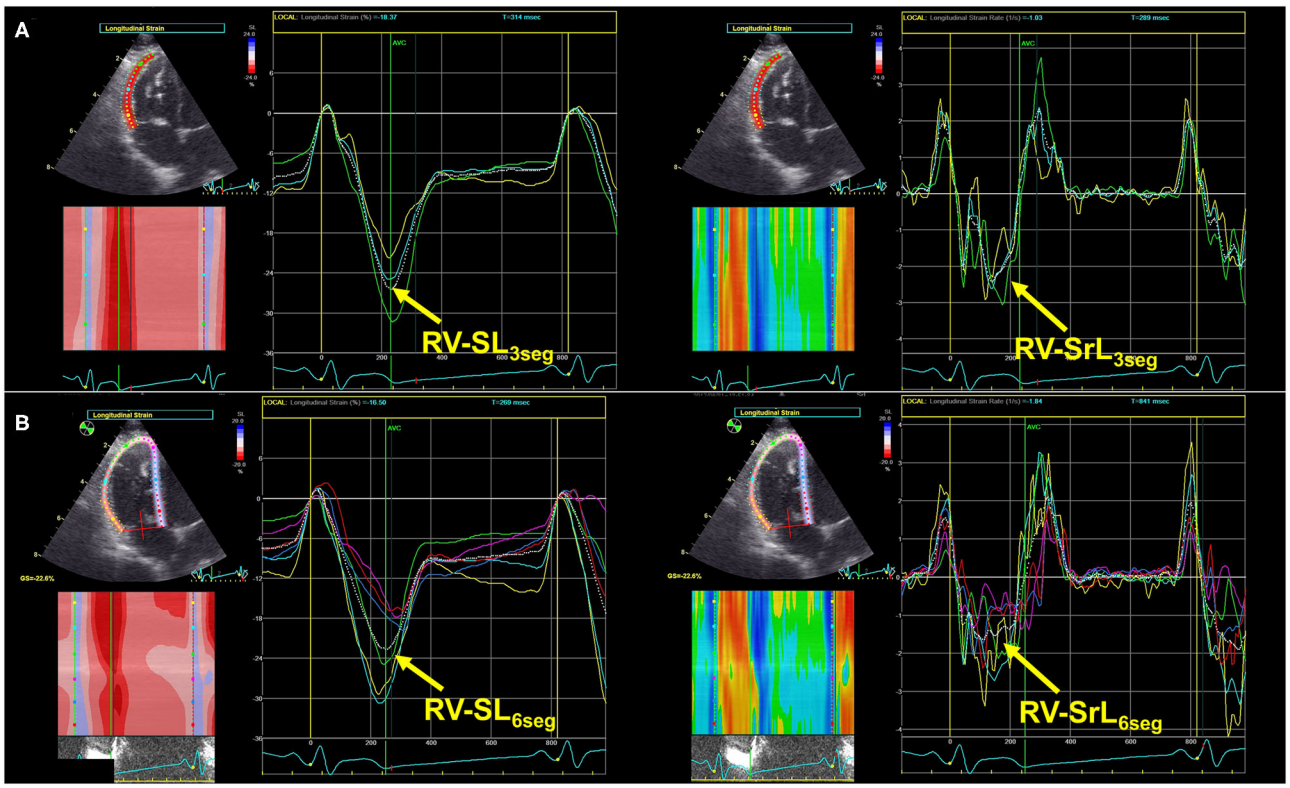

FIGURE 2 | Right ventricular longitudinal strain (RV-SL) and strain rate (RV-SrL) assessed by two-dimensional speckle tracking echocardiography. **(A)** RV-SL and RV-SrL obtained from right ventricular free wall ($RV\text{-}SL_{3seg}$ and $RV\text{-}SrL_{3seg}$, respectively). **(B)** RV-SL and RV-SrL obtained from the global right ventricle ($RV\text{-}SL_{6seg}$ and $RV\text{-}SrL_{6seg}$, respectively).

RV MPI was obtained from the tissue Doppler imaging-derived lateral tricuspid annular motion wave, and calculated by dividing the sum of isovolumic contraction and relaxation time by ejection time. Isovolumic contraction and relaxation time were calculated by subtracting the interval from the end of the late-diastolic tricuspid annular motion wave to the onset of the early-diastolic tricuspid annular motion wave by the duration of the systolic tricuspid annular motion wave. Ejection time was defined as the duration of the systolic tricuspid annular motion wave (22).

The PVRecho measured by the two methods was calculated using the following formulas (11, 13) (**Figure 1**):

$$\text{PVRecho} = \frac{\text{peak TR velocity (m/s)}}{\text{PV VTI (cm)}} \quad (6)$$

$$\text{PVRecho2} = \frac{[\text{peak TR velocity (m/s)}]^2}{\text{PV VTI (cm)}} \quad (7)$$

As an indicator of intrinsic RV systolic function, we measured RV longitudinal strain and strain rate (RV-SL and RV-SrL, respectively) using the two-dimensional speckle tracking echocardiography (2D-STE) method. All 2D-STE analyses were performed using the same offline workstation as that used for standard echocardiography. RV-SL and RV-SrL were obtained from the RV focus view using the left ventricular four-chamber algorithm (16, 17, 27). The region of interest for 2D-STE was determined by manually tracing the RV endocardial border. Manual adjustments were made to include and track the entire myocardial thickness over the cardiac cycle when necessary. When the automated software could not track the myocardial regions, the regions of interest were retraced and recalculated. RV-SL and RV-SrL were measured using only RV free wall analysis (3seg), performed by tracing from the level of the lateral tricuspid annulus to the RV apex (**Figure 2A**), and RV global analysis (6seg), performed by tracing from the lateral tricuspid annulus to the septal tricuspid annulus *via* the RV apex (i.e., both RV free wall and interventricular septum) (**Figure 2B**). RV-SL was reported as the absolute value of the negative peak obtained from the strain wave (16, 17, 27). The RV-SrL was obtained from the strain rate wave and was reported as the absolute value of the negative peak during systole (27–29).

Statistical Analysis

All statistical analyses were performed using commercially available software (R 2.8.1). Categorical data are expressed as absolute numbers and frequencies as percentages. Continuous data are reported as median (interquartile range).

TABLE 1 | Clinical characteristics of the study population.

Variables	Pulmonary hypertension probability			*P*
	Low	Intermediate	High	
Number	16	19	23	
Age (year)	11 (9.6–13.5)	11.6 (9.8–13.2)	13.3 (12.2–14.6)	0.056
Sex (male/female)	10/6	13/6	11/13	0.451
Body weight (kg)	5.1 (3.3–7.6)	4.4 (3.3–6.9)	4.8 (2.5–7.2)	0.769
ACVIM Stage (B1/B2/C, D)	8/5/3	5/11/3	0/7/16	0.004
R-CHF (present/absent)	0/16	0/21	10/13	<0.001
Heart rate (bpm)	121 (109–152)	136 (120–151)	149 (127–158)	0.350
Systemic arterial pressure				
Systole (mmHg)	126 (110–146)	136 (118–148)	135 (106–150)	0.451
Mean (mmHg)	92 (81–105)	98 (83–107)	96 (88–112)	0.832

Data are represented as median (interquartile range).
ACVIM, American College of Veterinary Internal Medicine; R-CHF, right-sided congestive heart failure.

Shapiro–Wilk test was performed to evaluate the normality of the data. Categorical indices were compared among the PH probability groups using Fisher's exact test. Continuous indices were compared among the PH probability groups using one-way analysis of variance with subsequent pairwise comparisons using Tukey's multiple comparison test for normally distributed data or the Kruskal–Wallis test with subsequent pairwise comparisons using the Steel–Dwass test for non-normally distributed data. All echocardiographic indices for right heart morphology and function were compared for the presence or absence of R-CHF using a Student's *t*-test for normally distributed data or the Mann–Whitney *U* test for non-normally distributed data. Additionally, univariate and multivariate logistic regression analyses were performed to evaluate the association between the presence of R-CHF and echocardiographic indices for the right heart, including PVRecho. After adjusting for multicollinearity, variables with $P < 0.10$ in the univariate analysis, were entered into the multivariate analysis. Results of logistic regression analyses were recorded as adjusted odds ratios and their respective 95% confidence intervals (CI). Receiver operating characteristic curves were created to calculate the area under the curve (AUC), sensitivity, and specificity, and to determine the optimal cutoff values required for evaluating the presence of R-CHF. The AUC was considered to have high accuracy if it was >0.9, moderate accuracy if it was 0.7–0.9, and low accuracy if it was 0.5–0.7 (30). The optimal cutoff value was defined as the value that minimized the distance between the curve and the upper left corner in the receiver operating characteristic curve.

Intra-observer variability measurements were performed by a single observer who performed all echocardiographic measurements (YY). The echocardiographic indices assessed in this study were obtained from nine dogs (three dogs in each PH probability group). All measurements were performed on two different days with >7-day intervals using the same cardiogram and cardiac cycles. A second blinded observer (HKa) measured the same indices to determine interobserver variability using the same echocardiogram and heart cycles. Variability of intra- and inter-observer measurements was quantified by the coefficient of variation (CV), which was calculated using the following formula:

$$\text{CV}\ (\%) = \frac{(\text{standard deviation})}{(\text{mean value})} \times 100$$

Intra- and inter-class correlation coefficients (ICCs) were also used to evaluate measurement variability. Low measurement variability was defined as CV < 10.0, and ICC > 0.70.

Statistical significance was set at $P < 0.050$ for all the analyses.

RESULTS

Clinical Characteristics

Fifty-eight client-owned dogs with MMVD and TR were enrolled in this study. The dogs were of the following breeds: Chihuahua ($n = 15$, 22%), mixed breed ($n = 7$, 12%), Toy Poodle ($n = 6$, 10%), Shi Tzu ($n = 5$, 9%), Miniature Dachshund ($n = 3$, 5%), Maltese ($n = 3$, 5%), Miniature Schnauzer ($n = 3$, 5%), Papillon ($n = 2$, 3%), Pomeranian ($n = 2$, 3%), Cavalier King Charles spaniel ($n = 2$, 3%), Chinese Crested dog ($n = 2$, 3%), Norfolk terrier ($n = 2$, 3%), and one dog each from eight other breeds. Seventy-eight percent of dogs with MMVD received medical treatment from the referral hospital at the time of examination, which was either angiotensin converting enzyme inhibitors (low: $n = 9$; intermediate: $n = 11$; high: $n = 20$), pimobendan (low: $n = 4$; intermediate: $n = 9$; high: $n = 14$), sildenafil (low: $n = 0$; intermediate: $n = 2$; high: $n = 5$), loop diuretics (low: $n = 0$; intermediate: $n = 0$; high: $n = 4$), or a combination of these. The clinical characteristics and systemic blood pressure results are summarized in **Table 1**. Age, sex, body weight, and systemic arterial pressure showed no significant differences among the PH probability groups. The proportion of the ACVIM stage of MMVD and the presence of R-CHF was significantly associated with PH probability ($P = 0.004$ and $P < 0.001$, respectively).

Echocardiographic Variables for the Right Heart

Table 2 shows the results of the echocardiographic variables, including the 2D-STE indices. Regarding the morphological

TABLE 2 | Results of echocardiographic indices in dogs with myxomatous mitral valve disease and pulmonary hypertension probability.

Variables	Pulmonary hypertension probability			*P*
	Low	Intermediate	High	
RVIDd index (mm/kg$^{0.327}$)	6.3 (5.3–7.3)	5.8 (5.3–7.1)	7.7 (6.8–9.5)*†	<0.001
RVEDA index (cm^2/kg$^{0.624}$)	0.83 (0.73–0.96)	0.86 (0.75–0.96)	1.17 (1.00–1.33)*†	0.001
RVESA index (cm^2/kg$^{0.628}$)	0.43 (0.36–0.47)	0.43 (0.31–0.51)	0.57 (0.47–0.73)*†	0.003
PA/Ao	0.82 (0.76–0.86)	0.90 (0.83–0.97)*	0.93 (0.85–1.19)*	0.002
TAPSEn (cm/kg$^{0.284}$)	7.2 (6.1–7.5)	7.5 (6.9–9.3)	8.0 (6.6–9.1)	0.205
RV FACn (%/kg$^{-0.097}$)	54.9 (49.4–63.5)	61.1 (49.7–63.3)	57.6 (47.2–61.2)	0.551
RV s' (cm/s)	11.7 (9.6–12.8)	11.4 (9.5–12.8)	11.8 (8.6–16.1)	0.433
RV MPI	0.45 (0.32–0.62)	0.41 (0.33–0.53)	0.58 (0.40–0.69)	0.112
PV VTI (cm)	8.6 (6.8–10.7)	8.8 (6.9–10.6)	7.1 (5.3–8.3)*†	0.005
TR velocity (m/s)	2.7 (2.2–2.8)	3.2 (3.1–3.4)*	3.9 (3.5–5.0)*†	<0.001
PVRecho	0.27 (0.23–0.40)	0.35 (0.29–0.46)*	0.60 (0.48–0.80)*†	<0.001
PVRecho2	0.73 (0.51–1.08)	1.11 (0.99–1.38)*	2.46 (1.66–3.58)*†	<0.001
RV-SL$_{3seg}$ (%)	29.3 (26.6–34.8)	31.0 (26.6–32.5)	25.1 (22.6–30.0)†	0.049
RV-SrL$_{3seg}$ (%/s)	4.9 (3.6–6.9)	5.3 (3.8–8.4)	3.4 (2.8–6.1)	0.088
RV-SL$_{6seg}$ (%)	25.8 (20.9–29.8)	27.4 (24.2–32.2)	20.6 (15.0–25.0)*†	0.003
RV-SrL$_{6seg}$ (%/s)	3.7 (2.6–4.6)	3.9 (2.6–5.3)	2.9 (2.2–3.5)†	0.021

Data are represented as median (interquartile range).

3seg, only right ventricular free wall analysis; 6seg, right ventricular global analysis; PA/Ao, pulmonary artery to aortic diameter ratio; PVRecho, pulmonary vascular resistance estimated by echocardiography; PV VTI, velocity–time integral of the pulmonary artery flow; RV, right ventricular; RV FACn, RV fractional area change normalized by body weight; RV MPI, RV myocardial performance index; RV s', tissue Doppler imaging-derived peak systolic myocardial velocity of lateral tricuspid annulus; RVEDA index, end-diastolic RV area normalized by body weight; RVESA index, end-systolic RV area normalized by body weight; RVIDd index, end-diastolic RV internal dimension normalized by body weight; RV-SL, RV longitudinal strain; RV-SrL, RV longitudinal strain rate; TAPSEn, tricuspid annular plane systolic excursion normalized by body weight; TR, tricuspid valve regurgitation.

**Variables that was significantly different from the low probability group (P < 0.050).*

†Variables that was significantly different from the intermediate probability group (P < 0.050).

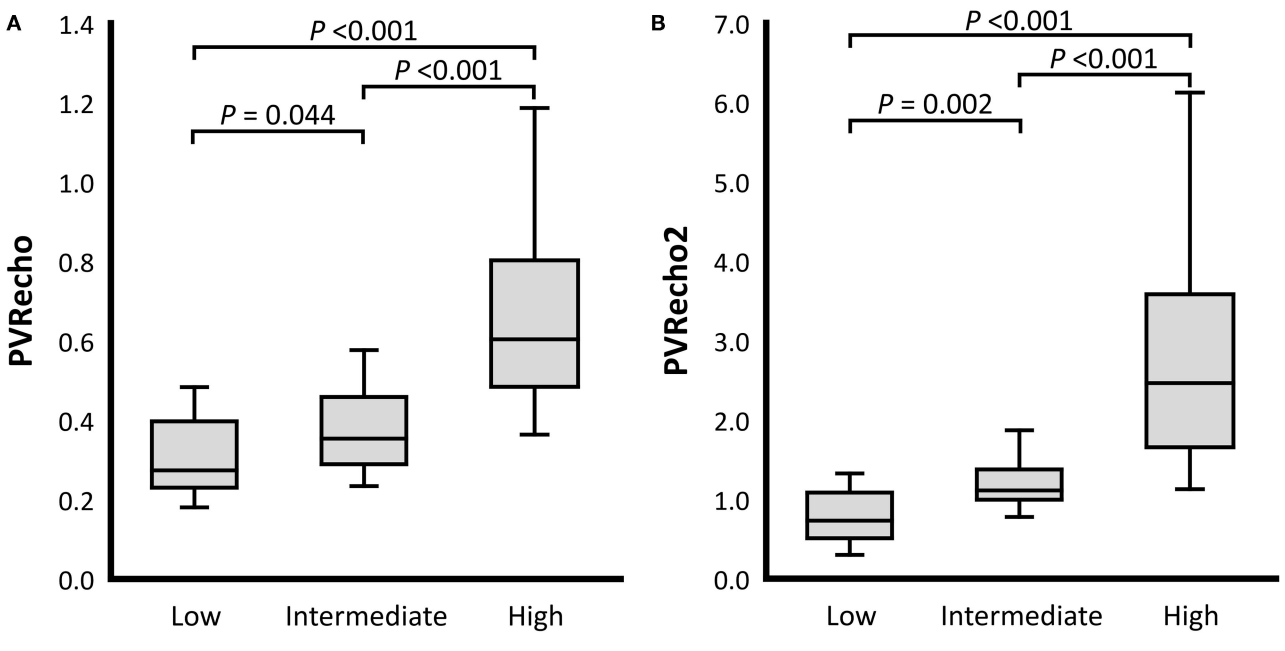

FIGURE 3 | Box and whisker plots of the pulmonary vascular resistance estimated by echocardiography (PVRecho). The bottom of the box is 25%, the middle line is the median, the top of the box is 75%, and the whiskers represent the range. **(A)** PVRecho. **(B)** PVRecho2.

TABLE 3 | Results of echocardiographic variables between the presence or absence of congestive heart failure.

Variables	Right-sided congestive heart failure		*P*
	Present	Absent	
RVIDd index (mm/kg$^{0.327}$)	10.0 (8.3–12.0)	6.7 (5.4–7.4)	<0.001
RVEDA index (cm^2/kg$^{0.624}$)	1.36 (1.13–1.67)	0.86 (0.74–1.01)	0.003
RVESA index (cm^2/kg$^{0.628}$)	0.73 (0.61–0.88)	0.45 (0.35–0.52)	0.003
PA/Ao	1.00 (0.89–1.27)	0.87 (0.81–0.92)	0.006
TAPSEn (cm/kg$^{0.284}$)	7.2 (6.0–8.5)	7.5 (6.7–8.3)	0.511
RV FACn (%/kg$^{-0.097}$)	49.2 (36.9–63.1)	58.8 (49.8–62.4)	0.113
RV s' (cm/s)	11.8 (8.5–17.4)	11.4 (9.3–13.6)	0.308
RV MPI	0.65 (0.34–0.96)	0.44 (0.37–0.58)	0.046
PV VTI (cm)	5.9 (4.5–7.9)	8.4 (6.8–9.7)	0.002
TR velocity (m/s)	5.0 (4.3–5.1)	3.1 (2.8–3.5)	<0.001
PVRecho	0.76 (0.62–1.00)	0.38 (0.29–0.48)	<0.001
PVRecho2	3.32 (2.80–5.03)	1.16 (0.84–1.62)	<0.001
RV-SL$_{3seg}$ (%)	25.5 (23.3–30.4)	28.8 (25.2–31.6)	0.395
RV-SrL$_{3seg}$ (%/s)	4.4 (2.7–6.4)	4.9 (3.3–6.8)	0.452
RV-SL$_{6seg}$ (%)	19 (13.3–24.3)	25.3 (20.9–28.4)	0.008
RV-SrL$_{6seg}$ (%/s)	2.4 (1.8–3.6)	3.4 (2.6–4.6)	0.017

Data are represented as median (interquartile range).
3seg, only right ventricular free wall analysis; 6seg, right ventricular global analysis; PA/Ao, pulmonary artery to aortic diameter ratio; PVRecho, pulmonary vascular resistance estimated by echocardiography; PV VTI, velocity–time integral of the pulmonary artery flow; RV, right ventricular; RV FACn, RV fractional area change normalized by body weight; RV MPI, RV myocardial performance index; RV s', tissue Doppler imaging-derived peak systolic myocardial velocity of lateral tricuspid annulus; RVEDA index, end-diastolic RV area normalized by body weight; RVESA index, end-systolic RV area normalized by body weight; RVIDd index, end-diastolic RV internal dimension normalized by body weight; RV-SL, RV longitudinal strain; RV-SrL, RV longitudinal strain rate; TAPSEn, tricuspid annular plane systolic excursion normalized by body weight; TR, tricuspid valve regurgitation.

TABLE 4 | Intra- and inter-observer measurement variability in echocardiographic variables assessed in this study.

Variables	Intra-observer			Inter-observer		
	CV (%)	ICC	*P*	CV (%)	ICC	*P*
RVIDd	3.2	0.97	<0.001	7.6	0.95	<0.001
RVEDA	4.0	0.99	<0.001	6.4	0.95	<0.001
RVESA	5.6	0.94	<0.001	7.6	0.96	0.001
PA/Ao	7.1	0.89	0.002	8.2	0.86	0.001
RV FAC	5.2	0.91	<0.001	7.5	0.67	0.001
TAPSE	3.5	0.90	<0.001	6.4	0.80	0.012
RV s'	2.7	0.97	<0.001	3.8	0.95	<0.001
RV MPI	9.1	0.86	0.002	12.5	0.72	0.044
PV VTI	3.8	0.98	<0.001	5.5	0.94	<0.001
TR velocity	0.9	0.99	<0.001	0.9	0.99	<0.001
PVRecho	3.7	0.99	<0.001	5.4	0.96	<0.001
PVRecho2	3.6	0.99	<0.001	5.4	0.97	<0.001
RV-SL$_{3seg}$	4.5	0.93	<0.001	5.2	0.92	<0.001
RV-SrL$_{3seg}$	6.4	0.95	<0.001	9.7	0.89	<0.001
RV-SL$_{6seg}$	5.6	0.91	<0.001	6.9	0.86	<0.001
RV-SrL$_{6seg}$	6.1	0.94	<0.001	8.0	0.93	<0.001

3seg, only RV free wall analysis; 6seg, RV global analysis; CV, coefficient of variation; ICC, intra- or inter-class correlation coefficients; PA/Ao, pulmonary artery to aortic diameter ratio; PVRecho, pulmonary vascular resistance estimated by echocardiography; PV VTI, velocity–time integral of the pulmonary artery flow; RV, right ventricular; RV FAC, RV fractional area change; RV MPI, RV myocardial performance index; RV s', tissue Doppler imaging-derived peak systolic myocardial velocity of lateral tricuspid annulus; RVEDA, end-diastolic RV area; RVESA, end-systolic RV area; RV-SL, RV longitudinal strain; RV-SrL, RV longitudinal strain rate; TAPSE, tricuspid annular plane systolic excursion; TR, tricuspid valve regurgitation.

indicators for the right heart, the RVIDd index, RVEDA index, and RVESA index were significantly higher in the high probability group than in the low and intermediate probability groups (RVIDd index: $P = 0.006$ [vs. low], $P < 0.001$ [vs. intermediate]; RVEDA index: $P = 0.002$ [vs. low], $P < 0.001$ [vs. intermediate]; RVESA index: $P = 0.006$ [vs. low], $P = 0.002$ [vs. intermediate]). Additionally, the PA/Ao ratio in the intermediate and high probability groups was significantly higher than that in the low probability group ($P = 0.049$ and $P = 0.005$, respectively).

For the RV functional variables, TAPSEn, RV FACn, RV s', and RV MPI showed no significant differences among the PH probability groups ($P = 0.205$, $P = 0.551$, $P = 0.433$, and $P = 0.112$, respectively). On the other hand, PV VTI in the high probability group was significantly lower than that in the low and intermediate probability groups (PV VTI: $P = 0.022$ and $P = 0.008$, respectively). TR velocity was significantly different among all PH probability groups ($P < 0.001$). PVRecho and PVRecho2 were also significantly different among all PH probability groups (PVRecho: $P = 0.044$ [low vs. intermediate], $P < 0.001$ [low vs. high and intermediate vs. high]; PVRecho2: $P = 0.002$ [low vs. intermediate], $P < 0.001$ [low vs. high and intermediate vs. high]) (**Figure 3**). Regarding the 2D-STE indices, RV-SL$_{3seg}$ in the high probability group was significantly lower than that in the intermediate probability group ($P = 0.049$). Additionally, RV-SL$_{6seg}$ in the high probability group was significantly lower than that in the low and intermediate probability groups ($P = 0.034$ and $P = 0.003$, respectively). Although RV-SrL$_{3seg}$ showed no significant difference among the PH probability groups, RV-SrL$_{6seg}$ in the high probability group was significantly lower in the intermediate probability group ($P = 0.023$).

Table 3 summarizes the echocardiographic indices for the right heart compared between the presence and absence of R-CHF. The comparison among the PH probability groups, RVIDd index, RVEDA index, RVESA index, and PA/Ao were significantly higher in dogs with R-CHF. Additionally, certain RV functional indices, including RV MPI, PV VTI, TR velocity, PVRecho, PVRecho2, RV-SL$_{6seg}$, and RV-SrL$_{6seg}$, were significantly different between dogs with and without R-CHF. However, TAPSEn, RV FACn, RV s', RV-SL$_{3seg}$, and RV-SrL$_{3seg}$ showed no significant differences between dogs with and without R-CHF.

The intra- and inter-observer measurement variability results are summarized in **Table 4**. For inter-observer variability, all variables assessed in this study showed low measurement variability. However, RV FAC and RV MPI did not meet the

TABLE 5 | Significant variables in logistic regression analysis to evaluate the association between right-sided congestive heart failure and echocardiographic variables.

Variables	Univariate analysis		Multivariate analysis	
	Non-adjusted odds ratio (95% CI)	*P*	Adjusted odds ratio (95% CI)	*P*
RVIDd index ($mm/kg^{0.327}$)	5.4 (1.7–16.5)	<0.001	3.2 (1.2–12.2)	0.036
RVEDA index ($cm^2/kg^{0.624}$)	2.1 (1.3–3.4)	<0.001		
RVESA index ($cm^2/kg^{0.628}$)	4.1 (1.8–9.5)	<0.001		
PA/Ao (0.1)	1.8 (1.2–2.6)	0.005		
RV FACn ($\%/kg^{-0.097}$)	1.1 (1.0–1.2)	0.029		
RV MPI (0.1)	1.5 (1.1–2.0)	0.019		
PV VTI (cm)	2.0 (1.2–3.3)	0.006		
TR velocity (m/s)	1.3 (1.2–1.6)	<0.001		
PVRecho (0.1)	4.5 (1.7–12.1)	0.003		
PVRecho2 (0.1)	1.3 (1.1–1.5)	0.001	1.2 (1.1–1.4)	0.026
RV-SL_{6seg} (%)	1.2 (1.0–1.3)	0.014		
RV-SrL_{6seg} (0.1 %/s)	1.1 (1.0–1.2)	0.018		

6seg, right ventricular global analysis; PA/Ao, pulmonary artery to aortic diameter ratio; PVRecho, pulmonary vascular resistance estimated by echocardiography; PV VTI, velocity–time integral of the pulmonary artery flow; RV, right ventricular; RV FACn, RV fractional area change normalized by body weight; RV MPI, RV myocardial performance index; RVEDA index, end-diastolic RV area normalized by body weight; RVESA index, end-systolic RV area normalized by body weight; RVIDd index, end-diastolic RV internal dimension normalized by body weight; RV-SL, RV longitudinal strain; RV-SrL, RV longitudinal strain rate; TR, tricuspid valve regurgitation.

criteria of low measurement variability based on CV < 10.0, and ICC > 0.70.

Logistic Regression Analysis

In the univariate analyses that evaluated the association between echocardiographic variables for the right heart and the presence of R-CHF, an association was observed between the presence of R-CHF and increased RVIDd index, RVEDA index, RVESA index, PA/Ao, RV MPI, TR velocity, PVRecho, and PVRecho2, and decreased RV FACn, PV VTI, RV-SL_{6seg}, and RV-SrL_{6seg} (**Table 5**). After adjusting for confounding factors, five indices, including RVIDd index, PA/Ao, RV MPI, PVRecho2, and RV-SL_{6seg}, were included in the multivariate model, and the RVIDd index and PVRecho2 remained significant in the multivariate analysis.

The results of the receiver operating characteristic curves of the significant variables in the univariate analysis are summarized in **Table 6**. The RVIDd index, RVESA index, TR velocity, PVRecho, and PVRecho2 had a high accuracy in detecting the presence of R-CHF, and the RVEDA index, PA/Ao, PV VTI, RV-SL_{6seg}, and RV-SrL_{6seg} had moderate accuracy, and the other variables had low accuracy.

DISCUSSION

This study was the first to evaluate the clinical utility of PVRecho in dogs with MMVD, classified according to the PH probability. Several echocardiographic variables such as TAPSEn, RV FACn, RV s', and RV MPI, showed no statistical significance among the PH probability groups; RV-SL_{3seg}, RV-SL_{6seg}, PV VTI, TR velocity, PVRecho, and PVRecho2 showed significant worsening with the increase in PH probability. Additionally, logistic regression analysis revealed a significant association between the presence of R-CHF and increased RVIDd index and PVRecho2. Our results suggest that PVR estimated by echocardiography may provide additional information for the diagnosis and stratification of PH in dogs with MMVD, reflecting the increase in PVR and associated RV adaptation and/or the progression to Cpc-PH.

In this study, PVRecho measured by the two methods was significantly higher as the PH probability increased. In particular, those in the high probability group showed substantially higher values compared to those in the low and intermediate probability groups. These results suggest that dogs with high PH probability might have an increase in PVR in addition to the increase in PAP. Furthermore, some dogs with high PH probability may have pulmonary arterial remodeling (i.e., the development of Cpc-PH). Higher PVRecho observed in this study may reflect increased PVR attributable to the significant pulmonary arterial remodeling and detect the Cpc-PH condition. However, since not all dogs have undergone histopathological examination, further studies that compare echocardiographic and histopathological findings are warranted in the future. Additionally, the PVR estimated by echocardiography was calculated with PV VTI, which reflects RV performance and TR velocity, which indicates RV afterload. Therefore, these indices might also reflect RV adaptation associated with increased PVR. Although TR velocity showed the same tendency as PVRecho, a previous study has reported that systolic PAP estimated by TR velocity showed poor agreement with that measured by catheterization (31), and ACVIM consensus stated that PH diagnosis by TR velocity alone should be avoided (1). Furthermore, our previous study reported that RV compensated for mild pressure overload by hyperactivation and decompensated for moderate-to-severe and chronic pressure overload in dogs with experimentally induced PH (27), suggesting that the pseudo-normalization of RV systolic function cannot be avoided as PH progresses. Therefore, the overall assessment of RV performance and afterload, such as PVRecho and PVRecho2, might be more useful for the clinical assessment of PH rather than the assessment using TR velocity and/or RV performance variables alone.

Logistic regression analysis in this study revealed a significant association between the presence of R-CHF and increased PVRecho2 with high AUC, sensitivity, and specificity. PVRecho was considered an independent factor for mortality in human patients with interstitial lung disease (12). Additionally, the development of Cpc-PH has been reported to be associated with RV failure and poor prognosis in patients with post-capillary PH (5, 32). Our results also suggest that increased PVR estimated by echocardiography may be a poor prognostic factor in dogs

TABLE 6 | Area under the curve and optimal cutoff of the significant variables in the univariate logistic regression analyses to detect the presence of right-sided congestive heart failure.

Variables	AUC (95% CI)	Cutoff	Sensitivity	Specificity
RVIDd index ($mm/kg^{0.327}$)	0.952 (0.887–1.000)	7.68	0.90	0.88
RVEDA index ($cm^2/kg^{0.624}$)	0.886 (0.726–1.000)	1.12	0.88	0.90
RVESA index ($cm^2/kg^{0.628}$)	0.902 (0.760–1.000)	0.54	0.82	0.90
PA/Ao (0.1)	0.776 (0.598–0.954)	0.96	0.70	0.82
RV FACn ($\%/kg^{-0.097}$)	0.684 (0.443–0.925)	51.3	0.70	0.74
RV MPI (0.1)	0.694 (0.470–0.917)	0.57	0.70	0.73
PV VTI (cm)	0.802 (0.657–0.947)	7.0	0.70	0.70
TR velocity (m/s)	0.907 (0.850–1.000)	4.52	0.80	0.96
PVRecho (0.1)	0.964 (0.921–1.000)	0.60	0.90	0.94
PVRecho2 (0.1)	0.974 (0.939–1.000)	2.46	0.90	0.94
$RV\text{-}SL_{6seg}$ (%)	0.748 (0.585–0.911)	22.40	0.70	0.72
$RV\text{-}SrL_{6seg}$ (0.1 %/s)	0.754 (0.582–0.926)	2.55	0.70	0.78

6seg, right ventricular global analysis; AUC, area under the curve; PA/Ao, pulmonary artery to aortic diameter ratio; PVRecho, pulmonary vascular resistance estimated by echocardiography; PV VTI, velocity–time integral of the pulmonary artery flow; RV, right ventricular; RV FACn, RV fractional area change normalized by body weight; RV MPI, RV myocardial performance index; RVEDA index, end-diastolic RV area normalized by body weight; RVESA index, end-systolic RV area normalized by body weight; RVIDd index, end-diastolic RV internal dimension normalized by body weight; RV-SL, RV longitudinal strain; RV-SrL, RV longitudinal strain rate; TR, tricuspid valve regurgitation.
Optimal cutoff was defined as that which minimized the distance between the curve and the upper left corner in the ROC curve.

with MMVD, reflecting the increased PVR and associated RV maladaptation and/or the progression to Cpc-PH. In this study, an increased RVIDd index was also associated with the presence of R-CHF with high AUC, sensitivity, and specificity, as well as PVRecho2. We previously described RV maladaptation against RV afterload in dogs with chronic PH and that RV dysfunction would induce RV dilatation to maintain RV cardiac output (27). Dogs with R-CHF in this study also showed RV dysfunction based on a decrease in RV-SL and RV-SrL and increased RV afterload based on TR velocity. Additionally, previous studies have reported that right heart dilatation is associated with the presence of R-CHF and shorter survival time (19, 33). Therefore, our results suggest that the PVRecho2 and RVIDd index may provide additional information to determine the presence of R-CHF in dogs with MMVD.

In our study population, PVRecho and PVRecho2 showed equivalent power for the stratification of PH probability and the detection of the presence of R-CHF. A previous human study reported that PVRecho2 was more reliable in estimating the catheterization-derived PVR than PVRecho in patients with substantially elevated PVR (11). Although not all dogs underwent right heart catheterization, our study results suggest that PVRecho calculated by both methods might be clinically useful for the diagnosis and stratification of PH in dogs with MMVD. However, the small study population of dogs with progressive PH and R-CHF might have affected the results in this study. Unfortunately, only a few dogs with post-capillary PH might progress to Cpc-PH. Further studies that accumulate more dogs with severe PH are expected in the future.

This study has several limitations. First, since not all dogs had undergone right heart catheterization, the definitive diagnosis of PH and the actual PVR value could not be completely clarified. Additionally, because not all dogs have undergone complete differential diagnosis, diseases that might increase PAP and/or PVR other than MMVD (i.e., pre-capillary PH) could not be completely ruled out (1). Second, few cases of misdiagnosis may have occurred in some dogs with R-CHF. Since none of the dogs underwent complete abdominal ultrasonography, we may not have identified some dogs with mild ascites. Third, some medications, especially pimobendan, sildenafil, and loop diuretics, might have affected RV function and hemodynamics. Especially, sildenafil, which would decrease PVR, might also affect our results of PVRecho. Finally, because the number of dogs with R-CHF in our study population was relatively small, the possibility of selection bias and insufficient power to detect statistical differences could not be excluded.

In conclusion, PVR estimated by echocardiography showed a significantly high value as the PH probability increased. These results suggest that these novel non-invasive values might be useful tools for the diagnosis and stratification of PH in dogs with MMVD. Additionally, multivariate logistic regression analysis revealed a significant association between the presence of R-CHF and increased PVRecho2 and the RVIDd index. Further studies that increase the study population and compare right heart catheterization- and echocardiography-derived PVR are warranted to validate the accuracy and utility of PVR estimated by echocardiography in the future.

DATA AVAILABILITY STATEMENT

The raw data supporting the conclusions of this article will be made available by the authors, without undue reservation.

ETHICS STATEMENT

The animal study was reviewed and approved by Ethical Committee for Animal Use of the Nippon Veterinary and Life Science University Veterinary Medical Teaching Hospital.

Written informed consent was obtained from the owners for the participation of their animals in this study.

AUTHOR CONTRIBUTIONS

RS provided the academic direction, performed the concept/design, data interpretation, critical revision of the manuscript, and approved the manuscript. YY performed the concept/design, data analysis/interpretation, drafting the manuscript, and critical revision of the manuscript. HKa performed the data analysis as a second observer. TS, TT, HM, and HKo performed data interpretation, critically revised the manuscript, and approved the manuscript. All authors contributed to the article and approved the submitted version.

FUNDING

This work was partially supported by the Japan Society for the Promotion of Science (JSPS) KAKENHI Grant Number 20K15667.

ACKNOWLEDGMENTS

The authors would like to express their deepest appreciation to Hatsumi Endo and Kana Yanagisawa for their technical assistance. This work was conducted at the Laboratory of Veterinary Internal Medicine, School of Veterinary Science, Faculty of Veterinary Medicine, Nippon Veterinary, and Life Science University in Tokyo, Japan. We would also like to thank Editage (www.editage.com) for English language editing.

REFERENCES

1. Reinero C, Visser LC, Kellihan HB, Masseau I, Rozanski E, Clercx C, et al. consensus statement guidelines for the diagnosis, classification, treatment, and monitoring of pulmonary hypertension in dogs. *J Vet Intern Med.* (2020) 34:549–73. doi: 10.1111/jvim.15725
2. Johnson L, Boon J, Orton EC. Clinical characteristics of 53 dogs with Doppler-derived evidence of pulmonary hypertension: 1992–1996. *J Vet Intern Med.* (1999) 13:440–7. doi: 10.1111/j.1939-1676.1999.tb01461.x
3. Kellihan HB, Stepien RL. Pulmonary hypertension in canine degenerative mitral valve disease. *J Vet Cardiol.* (2012) 14:149–64. doi: 10.1016/j.jvc.2012.01.001
4. Guazzi M, Naeije R. Pulmonary hypertension in heart failure: pathophysiology, pathobiology, and emerging clinical perspectives. *J Am Coll Cardiol.* (2017) 69:1718–34. doi: 10.1016/j.jacc.2017.01.051
5. Gerges C, Gerges M, Lang MB, Zhang Y, Jakowitsch J, Probst P, et al. Diastolic pulmonary vascular pressure gradient. *Chest.* (2013) 143:758–66. doi: 10.1378/chest.12-1653
6. Rezaee ME, Nichols EL, Sidhu M, Brown JR. Combined post- and precapillary pulmonary hypertension in patients with heart failure. *Clin Cardiol.* (2016) 39:658–64. doi: 10.1002/clc.22579
7. Tatebe S, Fukumoto Y, Sugimura K, Miyamichi-Yamamoto S, Aoki T, Miura Y, et al. Clinical significance of reactive post-capillary pulmonary hypertension in patients with left heart disease. *Circ J.* (2012) 76:1235–44. doi: 10.1253/circj.CJ-11-1288
8. Ibe T, Wada H, Sakakura K, Ugata Y, Yamamoto K, Seguchi M, et al. Combined pre- and post-capillary pulmonary hypertension defined by new criteria is worse prognosis group in patients with heart failure. *Eur Heart J.* (2020) 41: ehaa946-0174. doi: 10.1093/ehjci/ehaa946.2285
9. Hoeper MM, Bogaard HJ, Condliffe R, Frantz R, Khanna D, Kurzyna M, et al. Definitions and diagnosis of pulmonary hypertension. *J Am Coll Cardiol.* (2013) 62:D42–50. doi: 10.1016/j.jacc.2013.10.032
10. Abbas AE, Fortuin FD, Schiller NB, Appleton CP, Moreno CA, Lester SJ, et al. simple method for noninvasive estimation of pulmonary vascular resistance. *J Am Coll Cardiol.* (2003) 41:1021–7. doi: 10.1016/S0735-1097(02)02973-X
11. Abbas AE, Franey LM, Marwick T, Maeder MT, Kaye DM, Vlahos AP, et al. Noninvasive assessment of pulmonary vascular resistance by doppler echocardiography. *J Am Soc Echocardiogr.* (2013) 26:1170–7. doi: 10.1016/j.echo.2013.06.003
12. Yasui K, Yuda S, Abe K, Muranaka A, Otsuka M, Ohnishi H, et al. Pulmonary vascular resistance estimated by Doppler echocardiography predicts mortality in patients with interstitial lung disease. *J Cardiol.* (2016) 68:300–7. doi: 10.1016/j.jjcc.2016.02.025
13. Opotowsky AR, Clair M, Afilalo J, Landzberg MJ, Waxman AB, Moko L, et al. Simple echocardiographic method to estimate pulmonary vascular resistance. *Am J Cardiol.* (2013) 112:873. doi: 10.1016/j.amjcard.2013.05.016
14. Rhinehart JD, Schober KE, Scansen BA, Yildiz V, Bonagura JD. Effect of body position, exercise, and sedation on estimation of pulmonary artery pressure in dogs with degenerative atrioventricular valve disease. *J Vet Intern Med.* (2017) 31:1611–21. doi: 10.1111/jvim.14814
15. Keene BW, Atkins CE, Bonagura JD, Fox PR, Häggström J, Fuentes VL, et al. consensus guidelines for the diagnosis and treatment of myxomatous mitral valve disease in dogs. *J Vet Intern Med.* (2019) 33:1127–40. doi: 10.1111/jvim.15488
16. Suzuki R, Matsumoto H, Teshima T, Koyama H. Clinical assessment of systolic myocardial deformations in dogs with chronic mitral valve insufficiency using two-dimensional speckle-tracking echocardiography. *J Vet Cardiol.* (2013) 15:41–9. doi: 10.1016/j.jvc.2012.09.001
17. Yuchi Y, Suzuki R, Teshima T, Matsumoto H, Koyama H. Utility of tricuspid annular plane systolic excursion normalized by right ventricular size indices in dogs with postcapillary pulmonary hypertension. *J Vet Intern Med.* (2021) 35:107–19. doi: 10.1111/jvim.15984
18. Acierno MJ, Brown S, Coleman AE, Jepson RE, Papich M, Stepien RL, et al. consensus statement: guidelines for the identification, evaluation, and management of systemic hypertension in dogs and cats. *J Vet Intern Med.* (2018) 32:1803–22. doi: 10.1111/jvim.15331
19. Vezzosi T, Domenech O, Costa G, Marchesotti F, Venco L, Zini E, et al. Echocardiographic evaluation of the right ventricular dimension and systolic function in dogs with pulmonary hypertension. *J Vet Intern Med.* (2018) 32:1541–8. doi: 10.1111/jvim.15253
20. Visser LC, Scansen BA, Brown N V, Schober KE, Bonagura JD. Echocardiographic assessment of right ventricular systolic function in conscious healthy dogs following a single dose of pimobendan versus atenolol. *J Vet Cardiol.* (2015) 17:161–72. doi: 10.1016/j.jvc.2015.04.001
21. Gentile-Solomon JM, Abbott JA. Conventional echocardiographic assessment of the canine right heart: reference intervals and repeatability. *J Vet Cardiol.* (2016) 18:234–47. doi: 10.1016/j.jvc.2016.05.002
22. Rudski LG, Lai WW, Afilalo J, Hua L, Handschumacher MD, Chandrasekaran K, et al. Guidelines for the echocardiographic assessment of the right heart in adults: a report from the American Society of Echocardiography endorsed by the European Association of Echocardiography, a registered branch of the European Society of Cardiology, and the Canadian Society of Echocardiography. *J Am Soc Echocardiogr.* (2010) 23:685–713. doi: 10.1016/j.echo.2010.05.010
23. Visser LC, Im MK, Johnson LR, Stern JA. Diagnostic value of right pulmonary artery distensibility index in dogs with pulmonary hypertension: comparison with doppler echocardiographic estimates of pulmonary arterial pressure. *J Vet Intern Med.* (2016) 30:543–52. doi: 10.1111/jvim.13911
24. Lewis JF, Kuo LC, Nelson JG, Limacher MC, Quinones MA. Pulsed Doppler echocardiographic determination of stroke volume and cardiac output: clinical validation of two new methods using the apical window. *Circulation.* (1984) 70:425–31. doi: 10.1161/01.CIR.70.3.425

25. Visser LC, Sintov DJ, Oldach MS. Evaluation of tricuspid annular plane systolic excursion measured by two-dimensional echocardiography in healthy dogs: repeatability, reference intervals, and comparison with M-mode assessment. *J Vet Cardiol.* (2018) 20:165–74. doi: 10.1016/j.jvc.2018.04.002
26. Visser LC, Scansen BA, Schober KE, Bonagura JD. Echocardiographic assessment of right ventricular systolic function in conscious healthy dogs: repeatability and reference intervals. *J Vet Cardiol.* (2015) 17:83–96. doi: 10.1016/j.jvc.2014.10.003
27. Yuchi Y, Suzuki R, Kanno H, Teshima T, Matsumoto H, Koyama H. Right ventricular myocardial adaptation assessed by two-dimensional speckle tracking echocardiography in canine models of chronic pulmonary hypertension. *Front Vet Sci.* (2021) 8:727155. doi: 10.3389/fvets.2021.727155
28. Suzuki R, Yuchi Y, Kanno H, Teshima T, Matsumoto H, Koyama H. Left and right myocardial functionality assessed by two-dimensional speckle-tracking echocardiography in cats with restrictive cardiomyopathy. *Animals.* (2021) 11:1578. doi: 10.3390/ani11061578
29. Suzuki R, Matsumoto H, Teshima T, Koyama H. Effect of age on myocardial function assessed by two-dimensional speckle-tracking echocardiography in healthy beagle dogs. *J Vet Cardiol.* (2013) 15:243–52. doi: 10.1016/j.jvc.2013.07.001
30. Fischer JE, Bachmann LM, Jaeschke R, A. readers' guide to the interpretation of diagnostic test properties: Clinical example of sepsis. *Intensive Care Med.* (2003) 29:1043–51. doi: 10.1007/s00134-003-1761-8
31. Menciotti G, Abbott JA, Aherne M, Lahmers SM, Borgarelli M. Accuracy of echocardiographically estimated pulmonary artery pressure in dogs with myxomatous mitral valve disease. *J Vet Cardiol.* (2021) 35:90–100. doi: 10.1016/j.jvc.2021.03.003
32. Caravita S, Faini A, D'Araujo SC, Dewachter C, Chomette L, Bondue A, et al. Clinical phenotypes and outcomes of pulmonary hypertension due to left heart disease: Role of the pre-capillary component. *PLoS ONE.* (2018) 13:e0199164. doi: 10.1371/journal.pone.0199164
33. Visser LC, Wood JE, Johnson LR. Survival characteristics and prognostic importance of echocardiographic measurements of right heart size and function in dogs with pulmonary hypertension. *J Vet Intern Med.* (2020) 34:1379–88. doi: 10.1111/jvim.15826

Conflict of Interest: The authors declare that the research was conducted in the absence of any commercial or financial relationships that could be construed as a potential conflict of interest.

Publisher's Note: All claims expressed in this article are solely those of the authors and do not necessarily represent those of their affiliated organizations, or those of the publisher, the editors and the reviewers. Any product that may be evaluated in this article, or claim that may be made by its manufacturer, is not guaranteed or endorsed by the publisher.